ADHESION PROPERTIES OF DLC AND TiO_2 THIN FILMS USING SCRATCH TEST METHODS

JAN MIKŠOVSKÝ*, PATRIK KUTÍLEK, JAROSLAV LUKEŠ, ZDENĚK TOLDE, JAN REMSA, TOMÁŠ KOCOUREK, FRANTIŠEK UHEREK, and MIROSLAV JELÍNEK

Czech Technical University in Prague, Faculty of Biomedical Engineering, nam. Sitna 3105, 272 01 Kladno, Czech Republic
jan.miksovsky@fbmi.cvut.cz

Keywords: Diamond-like-carbon (DLC), titanium dioxide (TiO_2), thin films, adhesion, scratch test, standards, standardization

1. Introduction

Diamond like carbon layers are widely used layers in many branches of the industry, including medicine where are used for various implants as biocompatible material. In each application adhesion is very important because after detachment of thin layers from basic materials it does not serve its purpose and remains of the layer could cause additional damage to surrounding tissue in live organism. Adhesion is an important parameter for every coating. There are more methods for its determination, but one of the most used methods is scratch test. Nowadays, micro and nano-scratch tests supplement the classic (macroscopic) scratch test, which is well described in literature.

The progressive load scratch test was seriously suggested for coating adhesion measurements by Perry[2,3], Steinmann and Hintermann[4], Valli[5], etc. Today, the method is widely used by the coating industry and development laboratories. Its usefulness as an adhesion and quality assessment method has been discussed[1,6–10]. The scratch test is generally accepted as a good and an efficient method for quality assessment of coated surfaces, but its use for coating-to-substrate adhesion assessment has been criticised by several authors[10,11].

The scratch test consists of pulling a diamond stylus over the surface of a sample under a normal force, which is increased either stepwise or continuously until failure is observed. The normal load at which this happens is called the critical normal load. It is generally accepted that the test is suitable for coatings of thickness ranging from 0.1 to 20 μm. The scratch test procedures are described in the European, USA and Japan or international standards, which are transposed into the Czech standards. The standards are designed for wide range of different coating materials. Most important standards for quantitative single point scratch testing are:

Czech Republic:

- DIN EN 1071-3 and ČSN EN 1071-3 (727570) – Advanced technical ceramics coatings – Determination of adhesion and other mechanical failure modes.

International:

- ISO 20502 Fine ceramics – Determination of adhesion of ceramic coatings by scratch testing
- ISO N269 (Working Draft) – Fine ceramics coatings – Determination of adhesion.

USA:

- ASTM C1624 (C1624-05) Ceramic coatings – Determination of adhesion and other mechanical failure modes.

Japan:

- JAS JIS R Thin films on glass Substrates – Determination of adhesion.

There are more standards for various materials mainly for paints, varnishes and various polymers.

The types of the failure which are often observed in the scratch test depend critically on the properties of substrate and coating. The material response to loading conditions has been divided into three independent phases by Holmberg[13]. Phase one represents the ploughing of a stylus in the substrate material. The substrate material is deformed by plastic or elastic deformation and a groove is formed. The phase two represents the bending and drawing of a freestanding coating. The bending movements cause stresses and stress release in the coating when drawn between the surfaces. In this phase, the work done for overcoming friction is considered.

The phase three represents pulling and spalling the coating from one point on the surface when its other part is fixed. The increasing pulling force results in cracks at the place of maximum tensile stress. The formation of cracks in the groove of a scratch tester has been shown by e.g. (ref.[1,10,12,14–16]). They can typically be described as angular cracks, parallel cracks, transverse semi-circular cracks, coating chipping, coating spalling and coating breakthrough.

2. Experimental part

Both types of layers DLC and TiO_2 were prepared by Pulsed Laser Deposition with excimer laser with KrF filling (λ = 248 nm and pulse τ = 20 ns).

For DLC layers we used following deposition conditions: Basic substrate was silicon wafer Si(111), pressure in

Table I
Laser energy density used for DLC layer synthesis, number of pulses and measured thicknesses

Sample	Energy density [J cm^{-2}]	Num. pulses [–]	Thicknesses [nm]
DLC-1	10	2400	70 ÷ 80
DLC-2	6	4500	60 ÷ 75
DLC-3	4	5600	60 ÷ 70
DLC-4	2,5	8000	60 ÷ 75

chamber before deposition $1 \cdot 10^{-4}$ Pa, pressure during deposition 0,25 Pa of argon atmosphere with gas flow 10 sccm, temperature 20 °C, target-substrate distance was 50 mm. High purity graphite was used as target material. Laser densities for ablation from target, number of pulses and achieved thicknesses are summarized in Tab. I.

Deposition conditions of TiO_2 layers were: Basic substrate was silicon wafer Si(111), pressure in chamber before deposition at least $1 \cdot 10^{-3}$ Pa, pressure during deposition (10 ÷ 18) Pa of oxygen atmosphere with gas flow around 10 sccm. Depositions were made utilizing radiofrequency discharge (RF) and the temperature during deposition was higher than room temperature due to RF, but less than 100 °C. The target-substrate distance was 40 mm. Pure titanium and pure rutile were used for target basic material. The deposition length was two thousand pulses. For more information see Tab. II.

Table II
Laser energy density used for TiO_2 layer synthesis, target material T-titanium, R-rutile, oxygen O_2 pressure and measured thicknesses

Sample	Energy density [J cm^{-2}]	Target material [nm]	Pressure O_2 [Pa]	Layers thicknesses [nm]
TIO_2-1	3,2	T	18	100 ÷ 120
TIO_2-2	3,2	T	10	65 ÷ 105
TIO_2-3	3,2	R	10	120 ÷ 125
TIO_2-4	3,2	R	18	130 ÷ 140

Mechanical profilometer Alpha-Step IQ (KLA co.) was used for thickness determination, each layer was measured at six places.

For determination of adhesions we used one classic macroscratch tester and two micro/nanoscratch tester. Macroscratch tester REVETEST, scratch tester (CSM co.), nanosclerometric head for scanning probe microscope Solver Next (NT-MDT co.) and Hysitron Triboindenter TI950 with nanoscratch transducer SN5-483-194. For details about testers see Tab. III.

Table III
Summary for load indenter type, load range and scratch length for measurement systems

System	Indenter type [diamond]	Load range	Scratch length
CSM Revetest	Rockwell	1÷200 N	30 mm
Hysitron TI950	Berkovich	Up to 10 mN	10 µm
NT-MTD nanosclerometry head	Berkovich	Up to 150 mN	100 µm

3. Results and discussion

Evaluations of thin films adhesion, which were prepared by PLD technique, were realized at three different devices.

The first system REVETEST (CSM co.) is the standard macroscratch tester which is compatible to CSN EN 1071-3. From this system we obtained normal force, depth of penetration, acoustic emission and friction coefficient and force. The system is equipped with optical microscope with possibility to obtain photography. We used acoustic emission to estimate delamination point and we visually confirmed it from the photography of the scratch. Additionally, we checked penetration force, where we got through the layer to the basic substrate. There was no problem with evaluation of DLC layers and we detected acoustic emission in the point of delamination resp. critical load (F_D), see Tab. IV and Fig. 1.

There were problems with acoustic emission in case of TiO_2 layers because of high counts of droplets in the layers, which was probably the cause of high acoustic emission from the start of the scratch test. Used testing conditions were following: speed 5 mm min^{-1}, loading rate 14 N min^{-1}, tip radius 200 µm for DLC layers. For TiO_2 layers tip radius was 400 µm. Two or more scratches on each sample were made and verified the obtained results.

The second device was Hysitron TI950. This system measures in micro and in nanoscale. In this case was not possible to use standards. Standards do not exist for nanolayers and the Berkovich tip. We obtained lateral force and lateral coordinates, normal force and normal coordinates as time dependency. Information about friction could be evaluated too. Imaging of scratch is provided with SPM technique with the same measuring stylus with contact force 1 µN. Every sample was measured three times with used force ranging from 0 to 3 mN and length of scratch 6 µm. Loading rate was 170 nm s^{-1}. Delamination was not observed in the scanned image. We could only see changes in lateral force from graph dependencies (example of DLC-1 and DLC-3 see in Fig. 1) in place corresponding to the penetration depth (the layers thicknesses). The layers had a good adhesion, which was conclud-

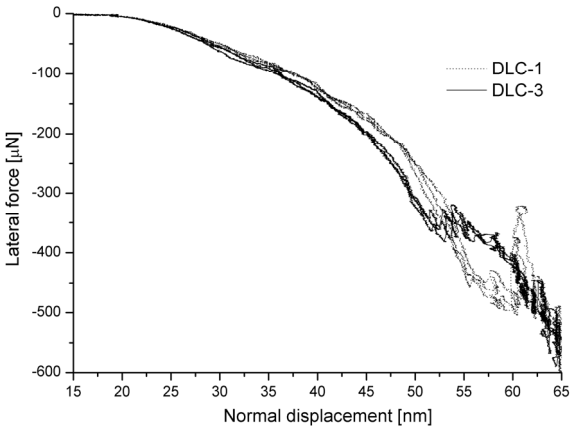

Fig. 1. **Example of dependency of lateral force on normal displacement**

Table IV
Summary of results from three used systems: F_D – delamination force, F_P – penetration force through layer to basic substrate

	CSM Revetest		Hysitron TI950		Nanosclerometric head	
Sample	F_D [N]	F_P [N]	F_D [mN]	F_P [mN]	F_D [mN]	F_P [mN]
DLC-1	6	8	NA	1.5	NA	63
DLC-2	9.5	13	NA	1.25	NA	>75
DLC-3	5	6.5	NA	1.1	NA	75
DLC-4	7.5	9.4	NA	1.25	NA	70
TIO_2-1	1	1	NA	0.75	NA	15
TIO_2-2	10	>25	NA	0.5	NA	33
TIO_2-3	>15	>15	NA	0.8	NA	39
TIO_2-4	4	NA	NA	NA	NA	18

ed from the stylus behaviour. After the stylus penetrated the layer to basic substrate the layer lifted up the stylus (see Fig. 1). We were not able to detect a critical force for TiO_2 and DLC layers, but only a change in the slope of lateral force dependency on a normal displacement corresponding to the layers thicknesses.

The third device we used was nanosclerometric head, which is an extension of AFM microscope Solver Next. This device provided us with the graphic information obtained by SPM technique with high resolution. For obtained images and made scratches same probe was used. Standards were not utilized, because for the Berkovich tip and the nanolayers standards do not exist. Two scratches with different loads were made on each sample. Length of scratches was 50 μm and loads were (0,5 ÷ 40) mN and (35 ÷ 75) mN for DLC layers and (0,5 ÷ 25) mN and (15 ÷ 50) mN for TiO_2 layers. Loading rate was 100 nm s^{-1}. For DLC layers changes were observed in behaviour of the layers. From certain used force the scratching depth grew rapidly, but this behaviour is not connected with adhesion to basic substrate, but with hardness of the layer itself and with the used probe sharpness. This happens because by AFM microscope Solver Next we measured residual depth and not the penetration depth. There was no such effect observed at TiO_2. Force F_P corresponds to penetrations force from the layer to basic substrate and was detected in both cases.

The macroscopic method for DLC layers gave us good results. The same method used for TiO_2 layers is complicated by influence of droplets in layer influencing acoustic emissions and by low contrast of scratch photography for some of these layers, which made difficult to interpret obtained imagines. Another problem with macroscopic scratch is high used force with combination of brittle substrate which caused damage of the sample for higher force than 25 N. This testing could be considered as destructive. For nanoscratch tests there are no classic marks for delamination or loss of adhesion as is described in various standards[12,15–18]. For Hysitron TI950 device, there is the clear change in lateral force/normal displacement dependency for all samples, but only on interface between the layers and basic substrate. Furthermore there is such dependency at TiO_2-1 sample where adhesion and strength of the layer was very low. The results from nanosclerometric head are closer to macroscopic scratch tester in meaning of needed force for penetration through the layer. Delamination or loss of adhesion was not observed for this method.

4. Conclusions

Four DLC and four TiO_2 layers prepared by PLD were measured on three different devices. The results from different devices did not match because of different measuring conditions and used tips, but we found some interesting results for other measurements of thin films by using described macro a nano scratch systems. The layers thickness determined by scratch testing was in an agreement with the measurement done with mechanical profilometer. Normal forces necessary to penetrate the layers were determined for all samples and devices used. Using CSM Revetest macroscopic scratch tester we were able to evaluate the measurement to determine the delamination force i.e. determine the quality of adhesion of nano layers in accordance with standard EN 1071-3.

This work was supported by grant of Ministry of Education, Youth and Sports of the Czech Republic MSM 6840770012 and by Grant Agency of Czech Technical University, Prague, No. SGS10/222/OHK4/2T/17.

REFERENCES

1. Bull S. J.: Surf. Coat. Technol. *50*, 1991.
2. Perry A.: Thin Solid Films 78, 1981.
3. Perry A.: Thin Solid Films 107, 1983.
4. Steinmann P., Hintermann H.: J. Vac. Sci. Technol. A3 (1985).
5. Valli J.: J. Vac. Sci. Technol. A3 (6) (1985).
6. Valli J.: J. Vac. Sci. Technol. A4 (6) (1986).
7. Valli J., Mäkelä U., Matthews A.: Surf. Eng. *2* (1) (1986).
8. Perry A.: Surf. Eng. *2* (3) (1986).
9. Bull S. J., Rickerby D., Matthews A., Leyland A., Pace A., Valli J.: Surf. Coat. Technol. *36* (1988).
10. Von Stebut J., Rezakhanlou R., Anoun K., Michel H., Gantois M.: Thin Solid Films 181 (1989).

11. Bromark M., Larsson M., Hedenquist P., Olsson M., Hogmark S.: Surf. Coat. Technol. 52 (1992).
12. European Standard EN1071-3: Advanced technical ceramics—methods of tests for ceramic coatings. Part 3. Determination of adhesion and other mechanical failure modes by scratch test.
13. Holmberg K.: Tribologia—Finn. J. Tribol. 19 (3) (2000).
14. Hedenquist P., Olsson M., Jacobson S., Hogmark S.: Surf. Coat. Technol. 41 (1990).
15. ASTM Standard C1624 (C1624-05): Ceramic coatings – Determination of adhesion and other mechanical failure modes.
16. International standards ISO 20502: Fine ceramics – Determination of adhesion of ceramic coatings by scratch testing
17. Japanese standard JAS JIS R: Thin films on glass Substrates – Determination of adhesion.
18. CSN EN 1071-3 (727570): Advanced technical ceramics coatings – Determination of adhesion and other mechanical failure modes.

J. Mikšovský[a,b], P. Kutílek[a], J. Lukeš[c], Z. Tolde[d], J. Remsa[a,b], T. Kocourek[a,b], F. Uherek[e], and M. Jelínek[a,b]
([a] Czech Technical University in Prague, Faculty of Biomedical Engineering, Kladno, [b] Institute of Physics ASCR, Prague, [c] Faculty of Mechanical Engineering, Czech Technical University in Prague, Prague, [d] Czech Technical University in Prague, Innovation Centre for Diagnostics And Application of Materials, Prague, Czech Republic, [e] International Laser Center, Bratislava, Slovakia): **Adhesion Properties of DLC and TiO_2 Thin Films Using Scratch Test Methods**

One of the important parameters of thin films made on various types of basic substrates is adhesion of these films to basic material. In this article, we focused on the study of the actual problem of adhesion of diamond-like-carbon films (DLC) and adhesion of titanium dioxide (TiO_2). The used deposition technique was Pulsed laser deposition (PLD) and the basic substrates were silicon wafers Si(111). We prepared testing samples of DLC with various deposition energies. The thicknesses of these tested films were several tens of nanometres. The TiO_2 testing samples were prepared with various deposition conditions and thicknesses in range of 60÷130 nanometres. On these samples we tested adhesion properties by various techniques based on scratch tests on various instruments in several different laboratory departments in the Czech Republic. For the individual instruments we observed and compared abilities of these systems to evaluate adhesion of thin films with thickness of 100 nanometres and less. For evaluation we used Czech, International and USA standards for ceramic and metallic materials.

EFFECT OF MICROSTRUCTURE OF Cu-Al_2O_3 COMPOSITE ON NANO-HARDNESS AND WEAR PARAMETERS

PAVOL HVIZDOŠ* and MICHAL BESTERCI

Institute of Materials Research, Slovak Academy of Sciences, Watsonova 47, 04001 Košice, Slovak Republic
phvizdos@imr.saske.sk

Keywords: Cu-Al_2O_3, ECAP, nanocomposite, wear

1. Introduction

Copper based materials are widely used in friction parts of machines, such as washers, bearing liners, etc. For these applications properties such as high strength and ductility, fatigue strength, wear resistance, etc., are necessary. To this end an approach of creating composites using hard dispersoid particles is often used[1].

Another way how such desirable properties can be achieved is creating very fine, submicron-grained microstructures[2]. Such microstructures can be prepared by inducing severe plastic deformation[3]. Very promising technique for preparation of these structures is ECAP (Equal Channel Angular Pressing) which results in very fine grained microstructure (nanostructure) by multiple pressings through the die[4].

The aim of the present study is to compare the hardness and wear of two copper based micro/nano-composites with 5 % alumina nanograins and different matrix grain sizes.

2. Experimental Materials

Reaction milling and mechanical alloying was used to prepare the samples. Cu powder with the calculated addition of Al was homogenized by attrition in oxidizing atmosphere. The distribution of the obtained CuO was uniform. Subsequent treatment at 750 °C induced the reaction of CuO with the added Al powder and led to the formation of Al_2O_3 particles. The remaining CuO was reduced by attrition in a mixture of H_2 + H_2O (rate 1:100). The powder was compacted using cold pressing and hot extrusion at 750–800 °C. This material was composed of micron sized grains of Cu and nanoparticles of Al2O3 and it is designated as Cu1.

Initial material with 5 vol.% Al_2O_3 was pressed through two right angled (90°) channels and transformed by the ECAP into a nanocomposite material. Resulting nanosized Cu-Al_2O_3 is denoted as Cu2.

3. Experimental Methods

Instrumented indentation was carried out on a nano-indentation tester TTX-NHT (CSM Instruments). Berkovich pyramid diamond tip was used in sinus mode loading of 5 Hz frequency and 5 mN load amplitude. Loads up to 100 mN were applied. The resulting load-penetration (P-h) curves were evaluated according to the analysis of Oliver and Pharr[5] and values of hardness and elastic modulus as functions of depth as well as elastic and plastic deformation energies were calculated. Up to 20 indentations were performed and the obtained data were statistically evaluated.

Wear testing was performed on a High Temperature Tribometer THT, (CSM Instruments), using ball-on-disk technique. The sample was fixed on a turntable with adjustable rotational speed. The tangential force exerted on the holder was measured and the coefficient of friction was recorded as function of distance/time/laps. Also the position of the holder was measured in order to evaluate the displacement due to material removed by wear. As friction partners steel balls with 6 mm diameter were used. The loading of 1 N was applied using a dead weight system. The nominal wear track radius was 2 mm, the sliding speed was set to 5 cm/s and the overall sliding distance was 100 m. Testing was done in air at room temperature in dry conditions. After the tests, both tribological partners (the steel ball and the sample) were observed using light and SEM microscopy. The depth and shape of the wear tracks were measured by a stylus profilometer (Mitutoyo SJ-201) at minimum three locations, the average wear track cross section area was calculated and subsequently the volume of the removed material was estimated. The wear rates were then expressed as the volume loss per distance and load (mm^3/m.N) and compared for both material systems.

4. Results

Microstructure of both materials was studied using TEM thin foils, in order to reliably identify the nanosized phases.

Fig. 1 shows TEM micrographs of the microstructures of experimental materials. Typical grain size in the material Cu1 was about 1–2 microns whereas in the material Cu2 it was from 100 to 200 nm.

Fig. 2 compares depth profiles of modulus of elasticity in Cu1 and Cu2 as measured by the instrumented indentation. In both cases these values were about 105 GPa at depths more than 1 μm, which corresponds to the elasticity of bulk copper. Smaller values at depths of penetration bellow 1 μm can be partly attributed to insufficient smoothness of the ground surface which was not highly polished. Another factor is the dislocation density, which during the testing increased under the indenter tip with increasing load until it reached the saturation point. The differences between the two materials were small, within the error range. Slightly higher values in Cu2 in smaller depths are caused by higher density of pre-existing dislocations in this highly plastically deformed material.

The difference in the case of hardness values was more pronounced (Fig. 3). Here, in both materials, the hardness start at higher values but also with very high scatter, which is caused by errors of measurement at very low loads and depths. For depths above 400 nm, however, the data show clearly two different levels of hardness, 2.28 GPa and 2.69 GPa for Cu1 and Cu2, respectively. This difference is

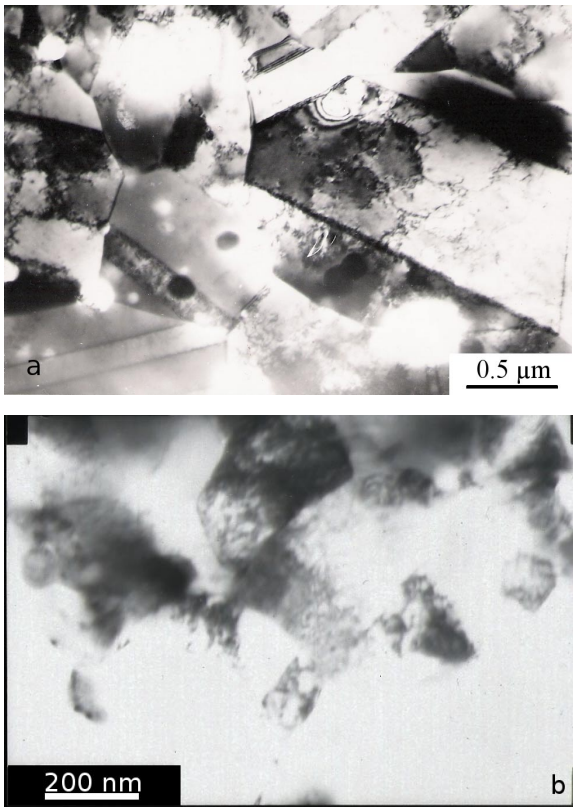

Fig. 1. **TEM micrographs, showing microstructure of (a) Cu1, and (b) Cu2**

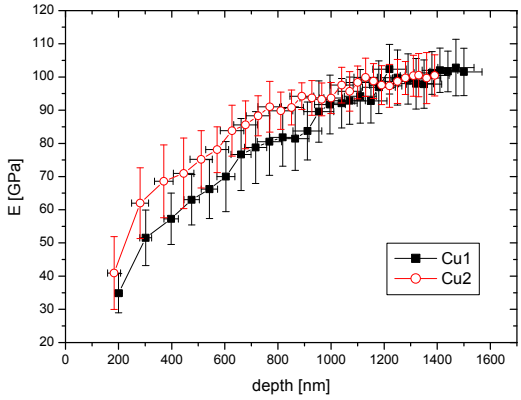

Fig. 2. **Modulus of elasticity vs depth for Cu1 and Cu2**

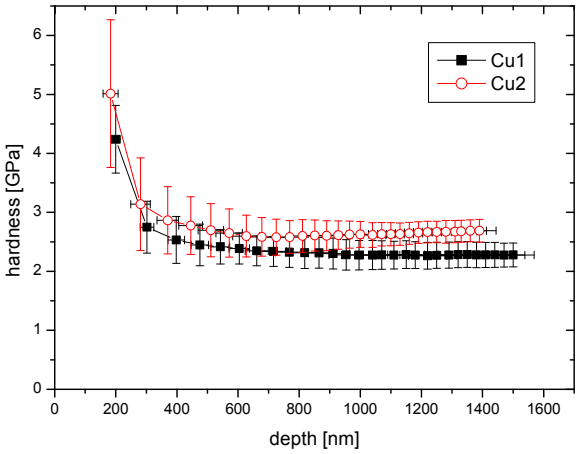

Fig. 3. **Depth profile of nano-hardness for both experimental materials**

statistically significant as it is greater than the scatter of the data.

From the load penetration (P-h) curves also the elastic (W_e), plastic, and total (W_t) energies of indentation were calculated. The differences between Cu1 and Cu2 are summarized in Table I. The elastic energy in indentation of Cu2 was higher than that of Cu1 even though its total indentation energy was lower. This behaviour was highly reproducible, as it is indicated by small scatter values (Tab. I).

It can be summarized that while the elasticity was in both cases very similar, the refinement of the matrix copper grains lead to a measurable increase of hardness and substantial increase of the ability for elastic recovery of the nanocomposite.

Table I
Indentation deformation energies

	Cu1	Cu2
W_t [nJ]	60.57 ± 2.11	47.30 ± 1.95
W_e [nJ]	5.57 ± 0.11	7.04 ± 0.17
W_e/W_t	0.092 ± 0.003	0.149 ± 0.005

Friction behaviour of both materials was in terms of coefficient of friction (COF) very similar (Fig. 4). At the beginning the COF started at low values, usually 0.12, which were very stable. After short running-in phase (2 to 10 meters of sliding distance) macroscopic failure of the surface began to take place and COF values rapidly rose up to 0.45–0.60, the values typical for steel-copper dry friction contact[6,7]. This level of friction then remained stable till the end of the test, up to 100 m sliding distance (nearly 8000 laps). The average values of COF in this wear regime were 0.55±0.02 for Cu1 and 0.58±0.03 for Cu2, respectively (Fig. 5).

Fig. 5 also compares the wear rates of both materials. It shows that the material Cu2 is about 3 times more wear resistant than the other one. This finding is analogous to literature data[8] for pure copper with submicro and nanocrystalline microstructures. Fig. 6 shows the wear tracks in both materials, photographed immediately after the test with the debris

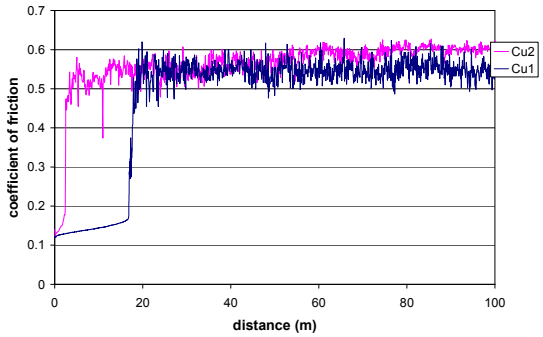

Fig. 4. **Coefficient of friction along the sliding distance**

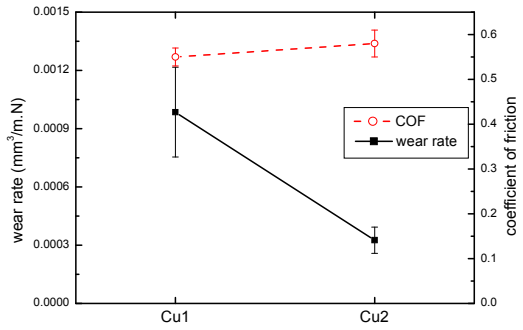

Fig. 5. **Coefficient of friction and wear rates of the experimental materials**

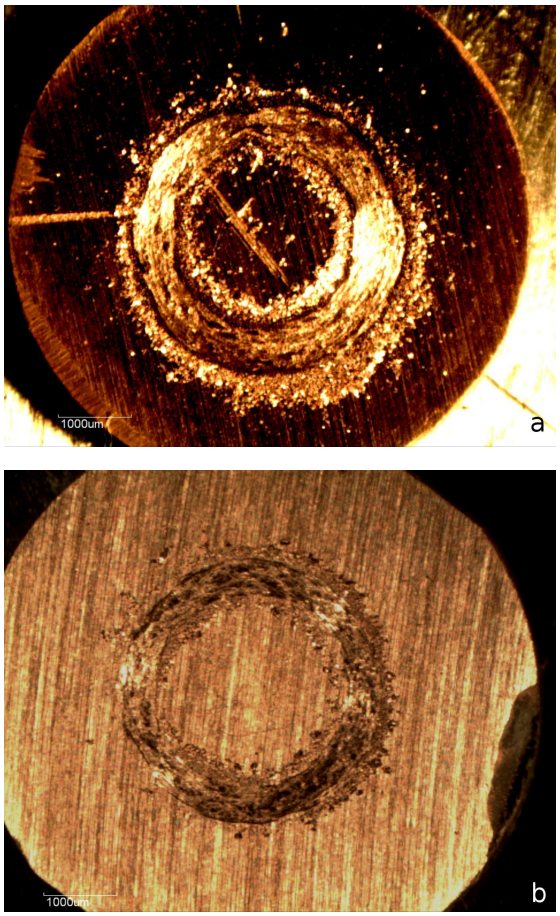

Fig. 6. **Wear tracks, together with wear debris, in Cu1 (a) and Cu2 (b)**

still present. The difference is immediately visible – the track in the Cu1 is larger and also the amount of wear debris around it is considerably greater (Fig. 6a) than in Cu2 (Fig. 6b).

The material was lost almost exclusively on the side of the copper discs; the steel balls were after the tests virtually intact. There were no circular worn caps present and in fact, it appears that part of the wear damage was due to adhesion of copper grains to the steel surface. This corresponds to the mechanism of copper transfer to the steel surface as it was established for coarse grained copper[9].

Details of the morphology of the worn areas in copper wear tracks are presented in SEM micrographs – Fig. 7. In both materials one can identify smooth and scarred areas, with presence of ductile and granular type of damage. The difference between the two materials is in the amount of the mentioned mechanisms. The worn surface of the material Cu1 (micro) is much smoother, in the material Cu2 granular features and fine particles are more frequently observed. SEM analysis showed, that in the present conditions mechanisms of 'mild' wear, as described in[8,10], were typical for both materials.

It can be concluded that the wear mechanisms are in both materials qualitatively the same, but the material with coarser grains contains more ductile damage.

5. Conclusions

Two Cu + 5 % Al_2O_3 composites with different size of the matrix grains were prepared. The hardness and elasticity was measured by instrumented nanoindentation, wear testing was carried out using pin-on-disc method and the friction and wear properties of both materials were compared. The results indicate that while both materials retained basically equal modulus of elasticity, corresponding to ordinary copper, the material with finer grains was significantly harder. The friction coefficients in both cases were very similar, corresponding to copper-steel sliding contact. The wear rates as well as the micrographic analyses indicate that in both cases mild wear of copper took place. The values of wear rates in terms

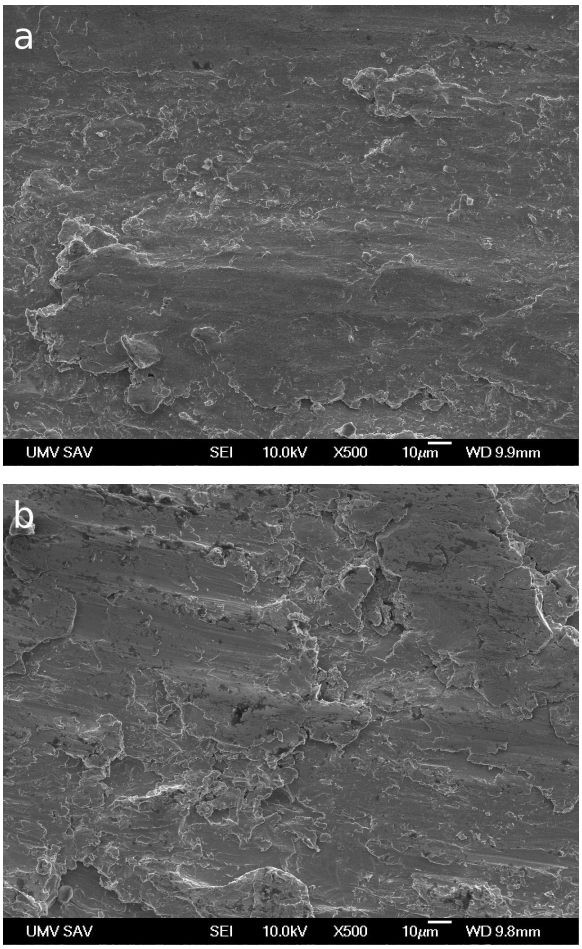

Fig. 7. **Details of wear tracks– (a) Cu1, (b) Cu2**

of the volume loss, however, were markedly different. It was shown that by ECAPing (i.e. by modification of microstructure – refinement of grains and introduction of the dislocations) the hardness and wear resistance can be improved significantly.

This work was realized within the frame of the project „Centre of Excellence of Advanced Materials with Nano- and Submicron-Structure", which is supported by the Operational Program "Research and Development" financed through European Regional Development Fund. The experiments could be carried out thanks to the projects VEGA 2/0120/10, 2/0025/11 and APVV-0520-10.

REFERENCES

1. Besterci M., Kováč L.: Int. J. Mater. Product Technol. *18*, 26 (2003).
2. Gleiter H.: Nanostruct. Mater. *1*, 1 (1992).
3. Valiev R. Z., Krasilnikov N. A., Tsenev N. K.: Mater. Sci. Eng., A *137*, 35 (1991).
4. Besterci M., Kvačkaj T., Kočiško R., Sülleiová K.: Int. J. Mater. Product Technol., in press.
5. Oliver W. C., Pharr G. M.: J. Mater. Res. *7*, 1564 (1992).
6. http://www.engineeringtoolbox.com/friction-coefficients-d_778.html
7. Marui E., Endo H.: Wear *249*, 582 (2001).
8. Sadykov F. A, Barykin N. P., Aslanyan I. R.: Wear, *225–229*, 649 (1999).
9. Syed Asif S. A, Bismas S. K., Pramila Bai B. N.: Scripta Met. et Mater. *24*, 1351 (1990).
10. Antoniou R., Borland D. W.: Mater. Sci. Eng. *93*, 57 (1987).

P. Hvizdoš and M. Besterci, *(Institute of Materials Research, Slovak Academy of Sciences):* **Effect of Microstructure of Cu-Al_2O_3 Composite on Nano-Hardness and Wear Parameters**

Two copper based composites with different grain size were studied: microCu-Al_2O_3 composite (grain size 1–2 microns), and nanoCu-Al_2O_3 nanocomposite prepared from microCu-Al_2O_3 by ECAP. This procedure resulted in 100–200 nm grain size.

Hardness and elastic modulus were measured by instrumented nanoindentation, the wear characteristics were evaluated using pin-on-disk method.

The results showed that the elastic modulus of the two materials was the same, similarly as the friction coefficient. However, it was found that by ECAPing the nanohardness increased due to refinement of the grains (increased density of grain boundaries) and thus the wear resistance improved by 200 %.

THE INFLUENCE OF ELEVATED TEMPERATURE ON COEFFICIENT OF FRICTION OF HVOF SPRAYED COATINGS MEASURED BY PIN-ON-DISC TEST

ROSTISLAV MEDLÍN* and ŠÁRKA HOUDKOVÁ

New Technologies - Research Centre, University of West Bohemia, Univerzitní 8, 306 14 Plzeň, Czech Republic
medlin@ntc.zcu.cz

Keywords: HVOF, coating, sliding, wear, pin-on-disc, CoF

1. Introduction

The friction between a piston, piston rings and a cylinder is responsible for almost 55 % of total power loss in engines. The decrease of friction in the piston area leads to a significant fuel saving and also to the emission reduction. The application of thermally sprayed coating is one possible way to decrease the friction and wear of engines.

From tribological point of view the engine system of piston, piston rings and cylinder is quite complicated. Together with the counterpart the piston ring makes a friction couple that should meet the requirements of low friction, wear and a long durability. During running, the system parts are submitted to the three-body abrasion, caused by the contamination of lubricant by solid particles. Compare to the rotational movement, the reciprocating linear movement is much more demanding due to sudden changes of direction, velocity, surface roughness and supply of lubricant. More to that, the piston rings surface is exposed to demanding chemical and thermal conditions. The study of the influence of elevated temperature on the sliding friction behavior of HVOF (High Velocity Oxygen Fuel) sprayed coatings are subject of this paper.

The technology of thermal spraying enables to create the surface coating approximately 50 μm thick, which provides the functional surface protection of the coated parts. The HVOF technology offers the possibility of creating the coatings of materials based on the principle of hardmetals with high wear resistance and favorable sliding properties. Such a combination predestinates the HVOF sprayed coatings for sliding applications, such as pistons of combustion engines, pumps and other hydraulic devices. In this application area they are used on a regular basis. By this reason, the wear resistance and the friction properties of these coatings were intensively studied under various conditions[1–4]. For severe wear applications, the HVOF sprayed hardmetal coatings are generally acknowledged as the best choice. Hardmetals offer an advantageous combination of wear and corrosion resistance with good friction properties. Some of them are also suited for elevated temperatures. They properties make them to be the good possibility for application in the piston-piston rings-cylinder system, as it was confirmed in previous works[5–7].

2. Experimental

Seven types of coating materials were chosen as potential candidates for engine parts application. The coating was sprayed by HP/HVOF JP-5000® (TAFA) spraying technology in the ŠKODA VÝZKUM s.r.o. in Plzeň, using the standard preparation procedure on the grit blasted substrate of carbon steel (ČSN 11 523) and the previously optimized spraying parameters. The average as-sprayed coatings thickness was 450 μm, surface grinding and polishing moves maximal 50 μm of thickness away. The coatings composition and basic mechanical properties are summarized in the Table I, the microstructures in the Fig. 2.

The coating sliding wear and friction properties were evaluated in the partner organization New Technology Center of University of West Bohemia in Plzeň (NTC ZČU), by the pin-on-disc test according to ASTM G-99, using High Temperature Tribometer produced by CSM Instruments SA. Even thought linear movement is more damaging than rotational movement, there can be seen relations between responses of testing materials and behavior of used materials.

The test was provided on the polished coating surface with the roughness Ra varying between 0,05–0,25. (see Table I) as original surface of piston rings used in engines. The testing used parameters are summarized in the Table II.

Working temperature of piston-rings in fuel-engine is calculated and measured about 350 °C (see Fig. 1) therefore temperature for piston-rings testing materials were used on that value.

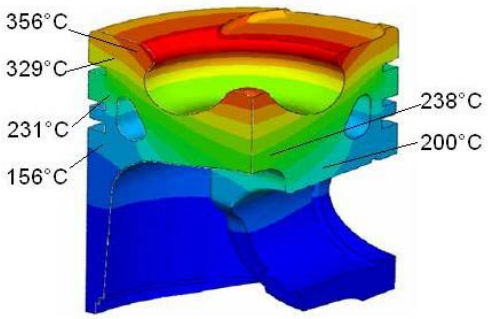

Fig. 1. **Temperature distribution in the piston**

The dry condition was chosen for the measurements to simulate the most demanding extreme situation of lack of lubricants that can cause the most severe wear of the coated parts. The results of influence of lubricants on the measured parameters can be found elsewhere[8].

Table I
Coatings mechanical properties

Coating	Surface roughness Ra	Micro-hardness HV0,3	Hardness HR15N
CoMoCrSi	0,13	705 ± 52	80,1 ± 1,9
NiCrMoWFe	0,05	420 ± 26	76,0 ± 1,7
WC-17%Co	0,25	1485 ± 88	90,0 ± 0,3
WC-20%CrC-7%Ni	0,10	829 ± 112	87,0 ± 0,9
Cr_3C_2-25%CoNiCrAlY	0,10	848 ± 30	85,3 ± 0,9
Cr_3C_2-25%NiCr	0,16	1030 ± 114	84,0 ± 0,5
Cr_3C_2-35%NiCr	0,14	811 ± 33	82,4 ± 0,9

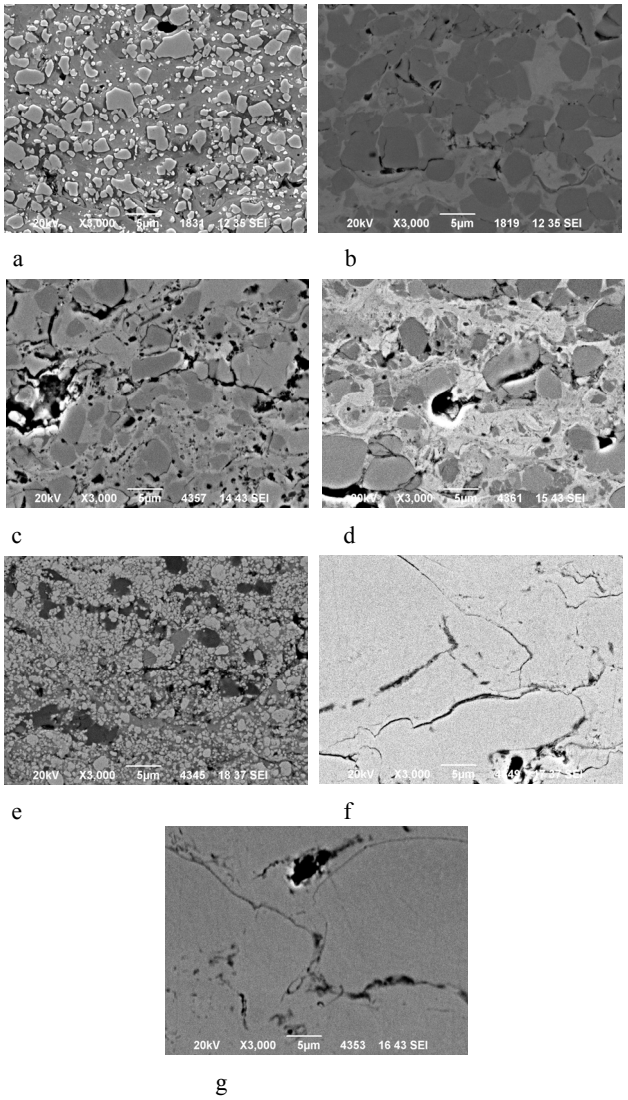

Fig. 2. **Microstructure of examined coatings a)WC-17%Co, b) Cr_3C_2-25%NiCr, c) Cr_3C_2-35%NiCr, d) Cr_3C_2-25%CoNiCrAlY, e) WC-20%CrC-7%Ni, f) CoMoCrSi, e) NiCrMoWFe**

Table II
Pin on disc test parameters

Pin	Al_2O_3 and Steel ball, ∅ 6 mm
Speed	0.1 m s^{-1}
Number of cycles	30 000
Pin load	10 N
Wear track diagonal	2, 3.5 and 5 mm
Temperature	20 °C, 350 °C
Lubrication	Dry

3. Results

The measured results of coefficient of friction (CoF) values are summarized in the Table III and the CoF detail progressions in dependence on the number of cycles are compared for all evaluated materials measured at room and elevated temperatures in the Fig. 3.

Table III
a) Pin on disc test CoF results for Steel Ball

Coating	CoF of Steel Ball	
	20 °C	350 °C
CoMoCrSi	0,710 ± 0,138	0,798 ± 0,010
NiCrMoWFe	0,732 ± 0	0,701 ± 0,006
WC-17%Co	0,780 ± 0,011	0,610 ± 0,008
WC-20%CrC-7%Ni	0,759 ± 0,002	0,611 ± 0,019
CrC-25%CoNiCrAlY	0,547 ± 0,002	0,630 ± 0,005
CrC-25%NiCr	0,713 ± 0,090	0,552 ± 0,004
CrC-35%NiCr	0,612 ± 0,029	0,614 ± 0,009

b) Pin on disc test CoF results for Al_2O_3 Ball

Coating	CoF of Al_2O_3 Ball	
	20 °C	350 °C
CoMoCrSi	0,685 ± 0,008	0,605 ± 0,138
NiCrMoWFe	0,666 ± 0	0,642 ± 0,013
WC-17%Co	0,364 ± 0,020	0,547 ± 0,026
WC-20%CrC-7%Ni	0,482 ± 0,0005	0,808 ± 0,007
CrC-25%CoNiCrAlY	0,684 ± 0,0005	0,616 ± 0,008
CrC-25%NiCr	0,671 ± 0,012	0,539 ± 0,0005
CrC-35%NiCr	0,605 ± 0,027	0,555 ± 0,017

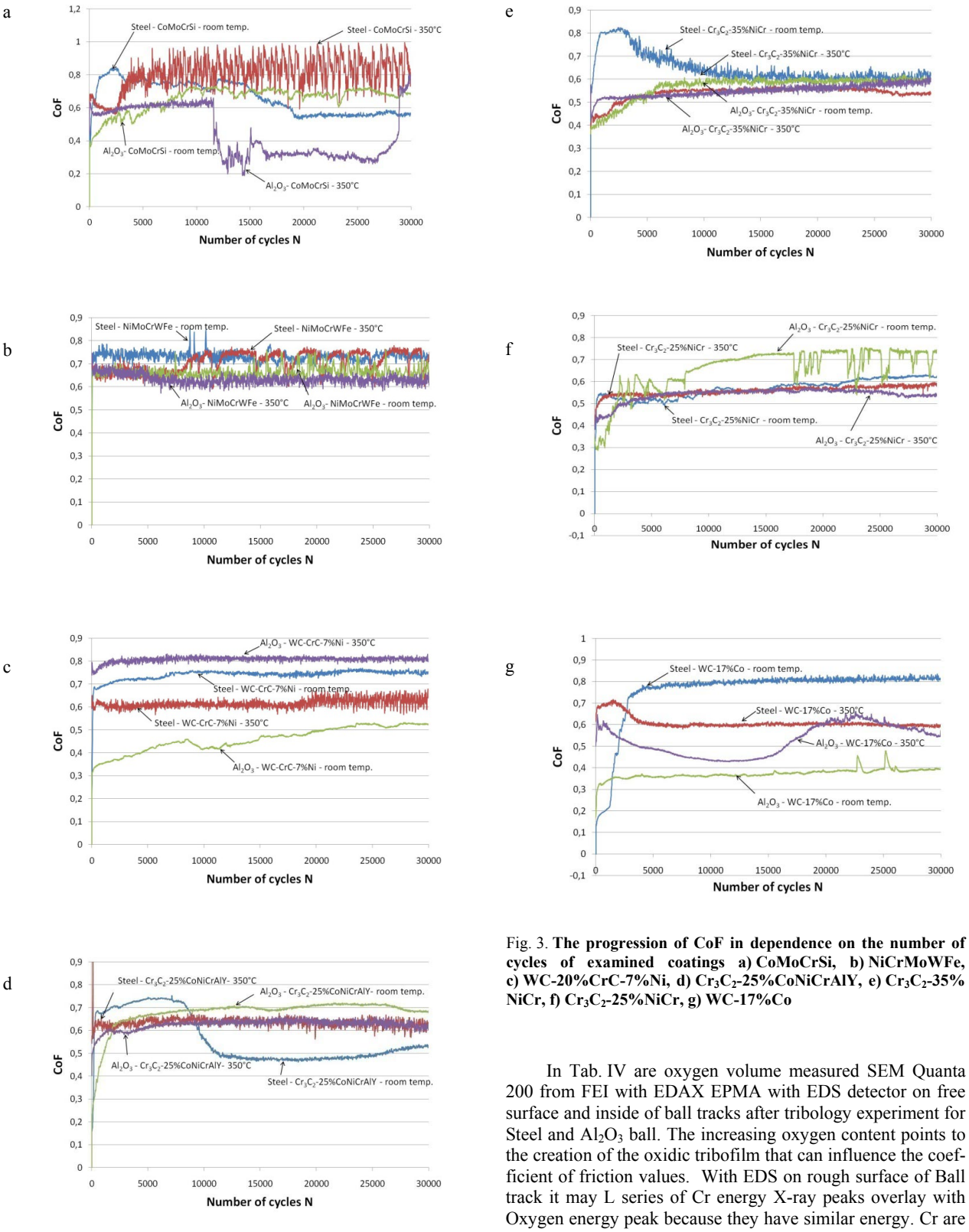

Fig. 3. **The progression of CoF in dependence on the number of cycles of examined coatings a) CoMoCrSi, b) NiCrMoWFe, c) WC-20%CrC-7%Ni, d) Cr_3C_2-25%CoNiCrAlY, e) Cr_3C_2-35% NiCr, f) Cr_3C_2-25%NiCr, g) WC-17%Co**

In Tab. IV are oxygen volume measured SEM Quanta 200 from FEI with EDAX EPMA with EDS detector on free surface and inside of ball tracks after tribology experiment for Steel and Al_2O_3 ball. The increasing oxygen content points to the creation of the oxidic tribofilm that can influence the coefficient of friction values. With EDS on rough surface of Ball track it may L series of Cr energy X-ray peaks overlay with Oxygen energy peak because they have similar energy. Cr are determined from K-series and L/K series intensity ratio are sensitive to surface roughness. Cr-Oxide film creation on surface was indicated in previous work[3].

Table IV
a) Oxygen volume in coatings for 20 °C

Coating	Oxygen volume [wt.%]		
	Free surface	Steel Ball	Al_2O_3 Ball
CoMoCrSi	0.00	17.03	3.43
NiCrMoWFe	0.00	0.00	0.19
WC-17%Co	1.42	12.89	1.30
WC-20%CrC-7%Ni	0.31	0.00	0.61
CrC-25%CoNiCrAlY	0.71	0.45	4.16
CrC-25%NiCr	1.68	0.72	39.79
CrC-35%NiCr	0.00	3.11	0.00

b) Oxygen volume in coatings for 350 °C

Coating	Oxygen volume [wt.%]		
	Free surface	Steel Ball	Al_2O_3 Ball
CoMoCrSi	2.01	2.46	3.25
NiCrMoWFe	0.00	0.00	12.23
WC-17%Co	3.07	7.64	5.79
WC-20%CrC-7%Ni	3.26	5.41	4.13
CrC-25%CoNiCrAlY	1.06	15.82	0.00
CrC-25%NiCr	1.80	2.39	8.10
CrC-35%NiCr	1.66	2.76	0.00

Wear mechanisms investigated by SEM were usual. For carbide materials there were marks of erosion of carbides from material and then abrasion from eroded carbides in wear track, in metal alloys abrasion and surface fatigue (Fig. 4).

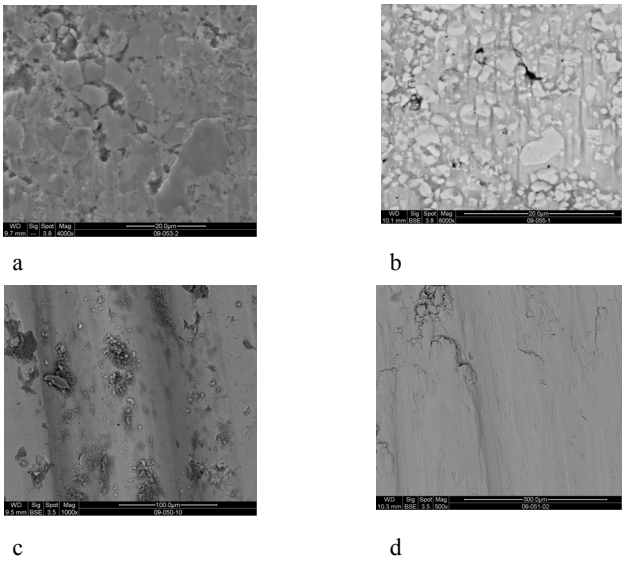

a b c d

Fig. 4. **Wear mechanisms of sprayed coatings observed by SEM. Erosion (a) and subsequently abrasion (b) of carbides in wear track for carbide materials and abrasion (c) and surface fatigue with adhesion, material transfer and pits (d) for metal alloys**

4. Discussion

The values and the progression of CoF change significantlyy with the increase of temperature. While for room temperature and Al_2O_3 counterpart the lowest CoF values shown the WC-based coatings and the CrC-based coatings shown the highest CoF values, for increased temperature it is backwards. The increased temperature causes the creation of oxidic film on the surface of CrC-based coatings that consist from Cr_2O_3, eventually $NiCr_2O_4$ (ref.[9]). Its CoF value range between 0,25–0,3 (ref.[10]), and it is well adhered to the coating surface. The WC-based coatings create at elevated temperature $CoWO_4$ a WO_3 oxides[9], that are poorly adhered to the coatings surface and tends to fall.

The CoMoCrSi coating on the CoF progression illustrates well the situation, where the creation of oxidical tribofilm causes the sudden decrease the CoF value. The tribofilm was at the end of the test ripped off, and the CoF increase immediately on its origin value. It is phenomenon that appears in the case of poorly adhered tribofilms[10].

Compare to the Al_2O_3 counterpart, the behavior in the contact with the steel counterpart changed especially for WC-based coatings, where the CoF is lower for higher temperature than for room temperature, while for Al_2O_3 counterpart it is contrariwise. The CrC-based coating had at elevated temperature similar behavior for Al_2O_3 and steel counterpart, the CoF values is in the range of 0,5–0,65, its progression is smooth, without significant fluctuation.

In the case of WC-CrC-Ni coating, the elevated temperature brings the increase of CoF for both counterparts. The created oxidic tribofilm does not have the expected positive effect as in the case of CrC-based coatings.

The NiMoCrWFe coating has stable behavior in all conditions. Due to its relatively low hardness it can be assumed, that the CoF value is determined more in consequence of plastic deformation during counterpart movement, and the counterpart material and surrounding temperature has not a big influence.

5. Conclusion

The measured results show that the presumption beneficial influence of Cr content in the coatings composition on their frictional properties can be confirmed only for hardmetal coatings. All CrC-based coatings with Cr in the matrix show with elevated test temperature decrease of CoF value (in the case of Al_2O_3 counterpart), or at least the unchanged behavior. More than the absolute CoF value the CoF progression is considerable due to its potential to predict the behavior in the following cycles. The Cr_2O_3 – which is together with $NiCr_2O_4$ the most probable oxide[4,9] – adheres strongly to the coating's surface and it is in correlation with CoF values measured in this study – characterized by CoF values in between 0.25–0.5 (ref.[10]). The alloy coatings with Cr content – CoMoCrSi and NiCrMoWFe – show no difference in the friction behavior even if the oxide tribofilm was measured by SEM EPMA. The WC-based coatings both show the increase of CoF with increasing temperature. Their oxidation behavior is not propitious for the application at elevated temperature. The combined WC-CrC-Ni hardmetal does not fulfill the

expectations, its behavior is not exceed the simpler WC-based and CrC-based coatings. The alloy coatings does are either not enough wear resistant (NiMoCrWFe) or unstable in CoF progression (CoMoCrSi). With respect to the results it can be said that the application requirement mentioned in the beginning meet from the suggested candidates only CrC-based hardmetals and that can be recommended for application on piston rings.

This work was supported by the Ministry of Industry and Trade of the Czech Republic no. FT-TA5/07.

REFERENCES

1. Bolelli G., et al.: Surf. Coat. Technol. *200*, 2995 (2006).
2. Picas A., Forn A., Matthäus G.: Wear *261*, 477 (2006).
3. Houdková Š., Zahálka F., Kašparová M.: Mater. Sci. Forum *567-568*, 229 (2007).
4. Berger L.-M., et al.: *In Conf. Proc. Int. Thermal Spray Conf. & Exhibition ITSC 2004*, DVS-Verlag, 2004, p.10.
5. Barbezat G.: *International Thermal Spray Conference (2004) May 10–12, Osaka*, Japan, Thermal Spray 2004: Advances in Technology and Application, Ed. B. R. Marple, C. Moreau, Pub. ASM International, Materials Park, OH, USA, 2004.
6. Herbst-Dederichs C.: Thermal spray solutions for Engine Piston Rings, Thermal Spray 2003: Advancing the Science and Applying the Technology, *International Thermal Spray Conference (2003) 5-8 May, Orlando*, Florida, (B. R. Marple, C. Moreau, ed.). Pub. ASM International, Materials Park, OH, USA, 2003, pp. 129–138.
7. Rastergar F., Richardson D. E.: Surf. Coat. Technol. *90*, 156 (1997).
8. Houdková Š., Zábranská I., Zahálka F.: *Metal 2009, 19.-21.5. 2009, Hradec nad Moravicí*, p. 258–265.
9. Berger L.-M., Zieris R., Saaro S.: *Conf. Proc. Int. Thermal Spray Confernce & Exhibition ITSC 2005, 2-4 May 2005, Basel*, Switzerland, Düsseldorf: DVS-Verlag, (2005), CD, pp. 969–976.
10. Buschnan B.: *Introduction to Tribology*, J. Wiley, New York 2002.

R. Medlín, and Š. Houdková *(New Technologies - Research Centre, University of West Bohemia, Plzeň, Czech Republic):*
The Influence of Elevated Temperature on CoF of HVOF Sprayed Coatings Measured by Pin-on-Disc Test

The pin-on-disc test according to ASTM G-99 was provided on selected thermally sprayed coatings to determine and describe their sliding wear behavior under elevated temperature. The progression of coefficient of friction was measured against two types of counterpart material, at room temperature and at 350°. After the test, the mechanisms of wear were studied by SEM and EDX. It was confirmed, that the content of Cr in the coatings is the most important factor causing the decrease of coefficient of friction with elevated temperature.